Annual Methodological Archive Research Review
http://amresearchreview.com/index.php/Journal/about
Volume 4, Issue 3 (2026)

Online ISSN 3007-3197
Print ISSN 3007-3189

http://amresearchreview.com/index.php/Journal/about

Green and Sustainable Synthesis of Bioactive Pyrimidine Derivatives Using Recyclable Nanocatalysts

Fatima Batool
Department of Applied Chemistry, Government College University Faisalabad
Email: fb446675@gmail.com

Muhammad Ashraf (Corresponding Author)
Department of Applied chemistry, Government college university faislabad
Email: ashrafalyani572@gmail.com

Muhammad Akhtar Abbas
Research scholar , Huazhong University of Science and Technology Wuhan, China
m.akhtarabbas410@gmail.com

Dr. Sharoon Mirza
Department of Pharmacy City University, Peshawar.
doctorsharoonmirza@gmail.com

Misha Aslam
Research scholar Government college university Faisalabad
mishaaslam4@gmail.com

ABSTRACT

Dihydropyrimidinones and thiones (DHPMs) are among the most valuable and useful pyrimidine skeletons in medicinal chemistry, but the traditional synthesis still requires strong mineral acids, volatile solvents and catalysts which cannot be recovered. The magnetic, sulfonic acid functionalised core–shell nanocatalyst, Fe_3O_4@SiO_2–SO_3H and its application in Biginelli condensation in the absence of solvent is reported. The catalyst was prepared by co-precipitation, silica coating (Stöber method), thiol grafting and peroxide oxidation, and was characterised by XRD, FTIR, TEM, N_2 physisorption, magnetometry and acid titration (1.12 mmol H^+ g^{-1}). Under optimized conditions (10 mg/mmol aldehyde, 90 °C, no solvent), 12 DHPMs (4a–4l) were isolated with an average yield of 92.0% (86–97% average) in 20-55 minutes. The atom economy of the model reaction was 87.8% and the E-factor was 6.6 (including recrystallisation solvent) compared to an E-factor of 63.2 for the conventional HCl/ethanol procedure. The catalyst was recovered using a hand magnet in approximately 20 s and could be recycled eight times, the yield decreasing from 95% to 86%. A hot filtration test suggested that the catalysis was of heterogeneous type. Two bacterial strains and the

Annual Methodological Archive Research Review
http://amresearchreview.com/index.php/Journal/about
Volume 4, Issue 3 (2026)

Online ISSN 3007-3197
Print ISSN 3007-3189
http://amresearchreview.com/index.php/Journal/about

MCF-7 breast cancer cells were used to screen the selected products. The 4k analog of the thiourea derivative exhibited the highest activity (IC_{50} = 9.8 ± 0.6 µM; MIC = 8 and 16 µg mL^{-1}). The approach provides a convenient and waste free pathway to bioactive pyrimidines.

Keywords— green chemistry; magnetic nanocatalyst; Biginelli reaction; dihydropyrimidinones; recyclable catalyst; anticancer activity

1. Introduction

One of the most prevalent heterocycles in biological systems is pyrimidine ring. It is the basis of the nucleobases cytosine, thymine and uracil, is also found in vitamins and coenzymes and is listed in a long list of marketed drugs (Lagoja, 2005). Synthetic pyrimidines have been reported to possess anticancer (Ghugal et al., 2021; Kaur et al., 2021), antimicrobial (Rahbar et al., 2021), antiviral and anti-inflammatory (Adebayo et al., 2021) activities and the structural variations on this ring continue to be reported (Rashid et al., 2021) with plenty of room to go. The 3,4-dihydropyrimidin-2(1H)-ones and thiones, obtained from the Biginelli reaction (Biginelli, 1891) have a particular relevance in this family. Their biological profile is broad (Kappe, 2000) and biological activity of small molecules targeted to a specific molecular target can be achieved using the scaffold, as demonstrated by the identification of monastrol, a DHPM that inhibits the mitotic kinesin Eg5 (Mayer et al., 1999).

The Biginelli reaction is also attractive from a process point of view. Three simple components, an aldehyde, a β-ketoester and urea or thiourea, are combined in one pot and water is the only by-product. They are now generally considered as tools for more sustainable synthesis (Cioc et al., 2014) and represent an example of multicomponent reaction of this type that is step economy and structurally diverse (Dömling et al., 2012). The original procedure, however, employs strong hydrochloric acid in refluxing ethanol, and generally suffers from modest yields for substituted aromatic aldehydes (Kappe, 1993). An N-acyliminium ion was later proposed as the key intermediate (Kappe, 1997), and this accounts for the high efficiency of acid catalysis. Lewis acids like indium(III) chloride (Ranu et al., 2000) and lanthanide triflates (Ma et al., 2000) were more effective in increasing yields and enabled solvent-free reactions, but are too costly, moisture sensitive and typically consumed during the work-up. Based on a wide survey of Biginelli catalysts, it is evident that many of the methods rely on homogeneous promoters, which are not easy to separate and reuse (Suresh & Sandhu, 2012).

Green chemistry provides guidelines for evaluating a synthetic approach. The Anastas and Warner (1998) and subsequent discussion (Anastas & Eghbali, 2010) of the 12 principles focus on the central feature of waste prevention and safer solvents and catalysis. These ideas are converted to number by atom economy (Trost, 1991) and the E-factor (Sheldon, 2012, 2017). Typically, the volume of solvents in a laboratory reaction is a large proportion of the waste stream and identifying alternative solvents is also a current research area (Jordan et al., 2022). A catalytic reaction that uses a solvent that can be readily recovered at the end of the reaction, thus resolving two of the main sources of waste.

Annual Methodological Archive Research Review
http://amresearchreview.com/index.php/Journal/about
Volume 4, Issue 3 (2026)

Online ISSN 3007-3197
Print ISSN 3007-3189
http://amresearchreview.com/index.php/Journal/about

Nanocatalysts are extremely beneficial as they combine features of both homogeneous and heterogeneous catalysis but are still in the form of a solid, which can be separated from the reaction products (Polshettiwar & Varma, 2010). If the nanoparticles are magnetic, separation can be achieved simply by using an external magnet, thereby eliminating the requirement for filtration and centrifugation, thus minimizing the losses of the catalyst (Baig & Varma, 2013; Polshettiwar et al., 2011). Usually the bare magnetite is coated with silica to prevent oxidation and aggregation, and the silica shell also contains hydroxyl groups which can be used for covalent attachment of catalytic functions (Gawande et al., 2013; Wang & Astruc, 2014).

A lot of reports break the various parts of such a system down individually. In this present work they have been analyzed together in a single workflow. A sulfonic acid functionalised magnetic core-shell catalyst was prepared and applied to 12 products in an optimized solvent-free Biginelli reaction, applied for reuse and leaching, and tested for 12 selected products for cytotoxic, and antibacterial activity, while calculating the green metrics against a conventional procedure. The goal was to demonstrate that a green approach to DHPMs could also provide compounds with interesting biological properties, and to determine which characteristics of their structure are important for that property.

2. Materials and Methods

2.1 Chemicals and biological materials

Iron(III) chloride hexahydrate, iron(II) chloride tetrahydrate, ammonium hydroxide (25%), tetraethyl orthosilicate (TEOS), (3-mercaptopropyl) trimethoxysilane (MPTMS), hydrogen peroxide (30%), toluene, ethanol, all aldehydes, ethyl acetoacetate, urea and thiourea were of analytical grade and were used as received. The human breast adenocarcinoma line MCF-7 was cultured in the standard culture medium containing 10% fetal bovine serum. The antibacterial test was carried out using Staphylococcus aureus (ATCC 25923) and Escherichia coli (ATCC 25922)..

2.2 Preparation of Fe_3O_4@SiO_2–SO_3H

Alkaline co-precipitation (Massart 1981) was used to prepare magnetite cores. $FeCl_3 \cdot 6H_2O$ (5.40 g, 20 mmol) and $FeCl_2 \cdot 4H_2O$ (1.99 g, 10 mmol) were dissolved in 100 mL of deoxygenated water under nitrogen gas at 80 °C followed by the dropwise addition of 25% ammonia to the reaction mixture under vigorous stirring. The black precipitate was stirred for 1 h, collected by a magnet, washed with water until neutral and then washed with ethanol. Following the Stöber approach (Stöber et al., 1968), 1.0 g of Fe_3O_4 was sonicated in an ethanol–water mixture (80 mL and 20 mL) for 20 min, 2 mL of NH_3 and 1.5 mL of TEOS were added and stirred for 12 h at 25 °C. The Fe_3O_4@SiO_2 particles (1.0 g) were then refluxed with MPTMS (1.5 mL, ~ 8 mmol) in dry toluene (50 mL) for 24 h under N_2. The thiol-functionalised solid was washed and then stirred in 30 mL of 30% H_2O_2 for 24 h at room temperature to oxidise the thiol groups, followed by 0.1 M H_2SO_4 for 12 h to ensure complete protonation, washed to neutral pH and dried at 60 °C under vacuum.

2.3 Catalyst characterisation

Powder X-ray diffraction was collected using CuKα radiation (λ = 1.5406 Å) in the range of 10° – 70° 2θ. Scherrer equation (Patterson 1939) was used to estimate crystallite size using (311) reflection. FTIR spectra were measured on KBr pellets from

Annual Methodological Archive Research Review
http://amresearchreview.com/index.php/Journal/about
Volume 4, Issue 3 (2026)

Online ISSN 3007-3197
Print ISSN 3007-3189
http://amresearchreview.com/index.php/Journal/about

4000 to 400 cm^{-1}. The particle size and shape were analyzed by transmission electron microscopy at least 200 particles were counted. Nitrogen adsorption–desorption isotherms were measured at 77 K and the surface area was calculated by the BET method (Brunauer et al., 1938). Vibrating sample magnetometry was used to obtain magnetisation curves at 300 K and CHNS analysis was used to determine the sulfur content. The acid capacity was determined by the ion exchange method and the released protons were titrated with 0.01 M NaOH solution. Filtrates of the reaction were analysed for content of iron and sulfur using ICP-OES.

2.4 General procedure for the Biginelli reaction

The aldehyde (1 mmol), ethyl acetoacetate (1 mmol), urea or thiourea (1.2 mmol) and the catalyst (10 mg unless specified) were added to a 10 mL tube, and stirred in an oil bath at 90 °C. Thin-layer chromatography (TLC) (n-hexane and ethyl acetate, 6:4) was used to monitor the progress. Once the aldehyde was used up, the mixture was allowed to cool down a little and 2 mL of hot ethanol was added, for dissolving the product and washing the catalyst. The catalyst was held at the wall of the tube with a magnet and the hot solution was decanted. The product was then cooled, filtered, washed with 2 mL of cold water and dried. No chromatography was used. The purity and identity were established by comparative analysis to reported data by melting point, FTIR and ^{1}H NMR and ^{13}C NMR (400 MHz and 100 MHz, DMSO-d_6). Optimisation reactions were performed in duplicate; the results, which were within 2% of each other, were averaged. For the comparison reaction (Table 1, entry 14), the aldehyde, ethyl acetoacetate and urea were refluxed in 10 mL of ethanol with two drops of concentrated HCl for 4 h.

2.5 Reusability and hot filtration tests

The catalyst was recovered after every run for the model reaction (benzaldehyde, ethyl acetoacetate and urea) with a magnet, rinsed with ethanol, dried at 60 °C for 2 hours and then weighed. For the subsequent runs, new substrates were used, with a loading adjusted to the amount recovered, to maintain the loading at 10 mg/mmol of aldehyde. In the hot filtration test, the catalyst was separated using a magnetic filter after 10 min and the filtrate was stirred for 20 min at 90 °C without the catalyst. Control reaction was performed for 30 min in the presence of catalyst.

2.6 Green metrics

The atom economy (AE) was determined by dividing the molar mass of the product by the sum of the molar masses of all reactants. The E-factor of the waste was determined as being the total mass of the waste/ mass of isolated product, including unreacted material, by-products and recrystallisation solvent, but excluding water and any recovered catalyst (Sheldon, 2017). Reaction mass efficiency (RME) was the product mass divided by the mass of reactants (Constable et al., 2002) and process mass intensity (PMI) was the total mass of the input divided by the mass of the products. The traditional comparison was made using 10 mL of ethanol for the reaction and 4 mL for recrystallisation and the yield of 68% from Table 1. The values are all for a scale of 1 mmol.

2.7 Cytotoxicity assay

MCF-7 cells were cultured in 96-well plates at the cell density of 5×10^3 cells per well. They were then treated with the test compounds (0.5-100 μM, DMSO <0.5%) for 48 h. The MTT assay (Mosmann, 1983) was used to determine viability and absorbance of

Annual Methodological Archive Research Review
http://amresearchreview.com/index.php/Journal/about
Volume 4, Issue 3 (2026)

Online ISSN 3007-3197
Print ISSN 3007-3189
http://amresearchreview.com/index.php/Journal/about

each well was read at 570 nm. Doxorubicin was the positive control. IC_{50} values were calculated using 4 parameter logistic regression.

2.8 Antibacterial assay

The minimum inhibitory concentration (MIC) was determined by broth microdilution following the guidelines of the CLSI M07 (Clinical and Laboratory Standards Institute [CLSI], 2018) with inoculum of 5×10^5 CFU mL^{-1} and incubation for 18–20 h at 37 °C and concentrations ranging between 2 and 256 µg mL^{-1}. Ciprofloxacin was used as the reference drug.

2.9 Statistics

Biological values are means ± standard deviations (SD) of three independent experiments. One-way ANOVA followed by Tukey's multiple comparison test was used to determine differences with $p < 0.05$ considered significant.

3. Results and Discussion

3.1 Structure and properties of the catalyst

The path towards the catalyst and towards the synthesis of the Biginelli reaction promoted by the catalyst is summarised in Figure 1. The structural characterisation is shown in Figure 2. The diffraction pattern of the uncoated cores contained six reflections at 30.1°, 35.5°, 43.1°, 53.4°, 57.0° and 62.6°, which are indexed to the (220), (311), (400), (422), (511) and (440) planes of cubic inverse-spinel magnetite. It was found that there were no changes after silica coating and sulfonation, the core was still crystalline. A broad hump was observed in the coated samples between 15° and 30° and is characteristic of the amorphous silica. The crystallite size obtained from the (311) reflection in the present study was 13.8 nm, which is in agreement with the TEM observation of the core diameter of 14 ± 3 nm. The coated particles were 26 ± 5 nm after coating, equivalent to a silica shell of 6 nm.

Annual Methodological Archive Research Review
http://amresearchreview.com/index.php/Journal/about
Volume 4, Issue 3 (2026)

Online ISSN 3007-3197
Print ISSN 3007-3189

http://amresearchreview.com/index.php/Journal/about

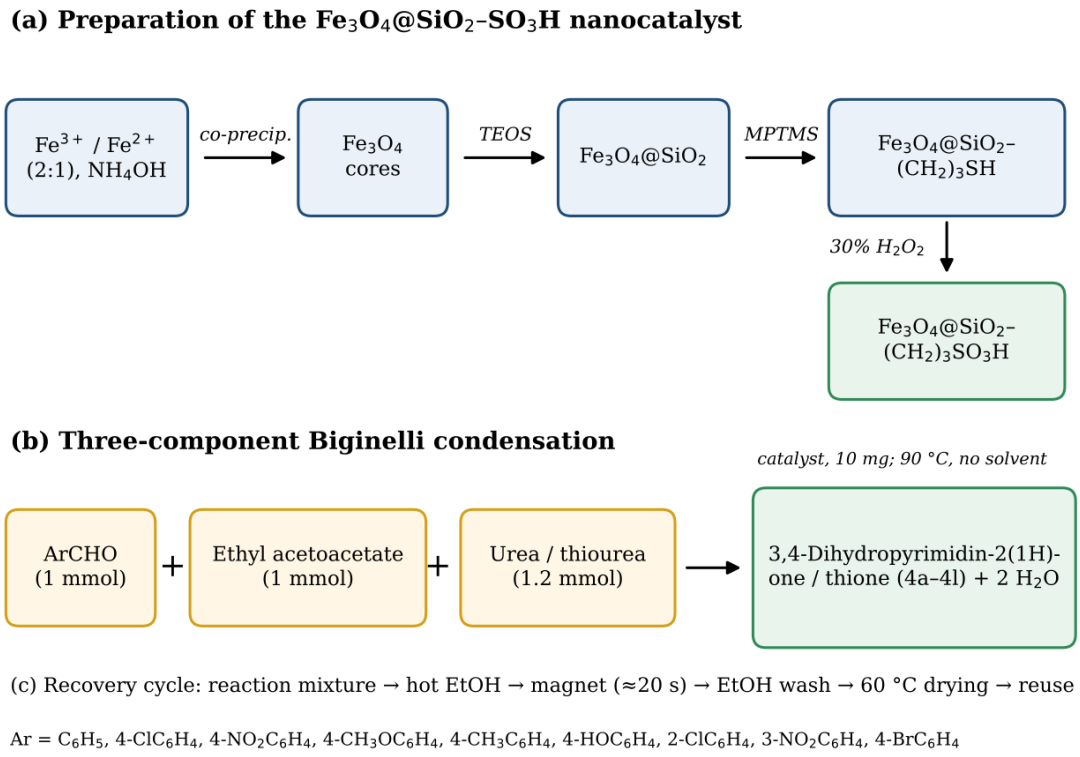

Figure 1. Preparation of the $Fe_3O_4@SiO_2–SO_3H$ nanocatalyst (a), the three-component Biginelli condensation studied here (b) and the recovery cycle (c).

The stepwise functionalisation was confirmed by the FTIR spectra. Fe–O and O–H bands were observed at 575 and 3420 cm^{-1}, respectively, and 1630 cm^{-1}, respectively, in all samples. The silica coating produced the Si–O–Si band at 1085 cm^{-1} as well as a weaker band at 800 cm^{-1}. Following grafting and oxidation, new bands were observed at 2930 cm^{-1} (C–H of propyl linker), and at 1185 cm^{-1} and 1035 cm^{-1} that are attributed to the asymmetric and symmetric S=O stretches of the sulfonic acid group. The S=O bands are slightly overlapping with the broad silica band, and thus are seen as shoulders to the higher wavenumber side of the silica band.

Annual Methodological Archive Research Review
http://amresearchreview.com/index.php/Journal/about
Volume 4, Issue 3 (2026)

Online ISSN 3007-3197
Print ISSN 3007-3189
http://amresearchreview.com/index.php/Journal/about

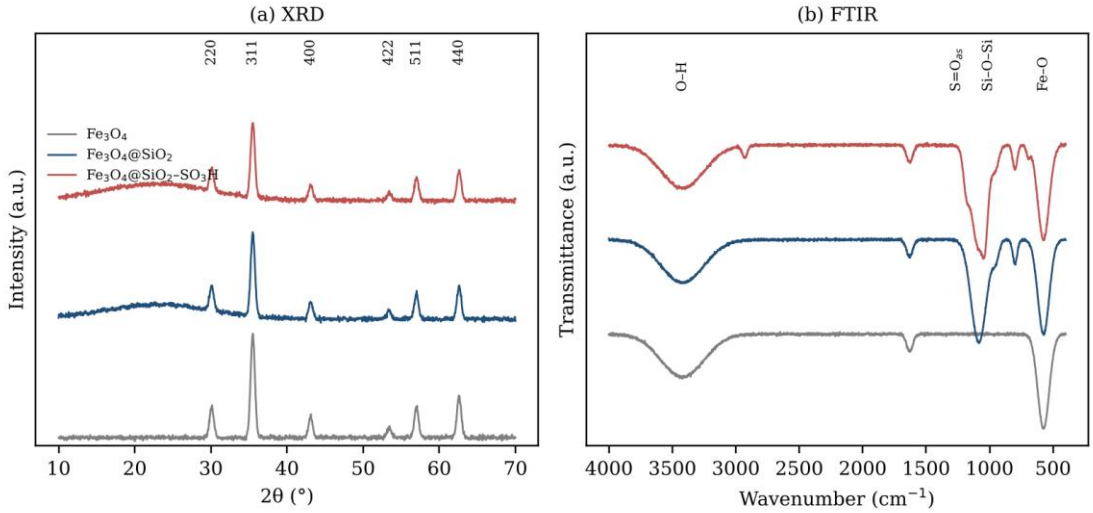

Figure 2. (a) X-ray diffraction patterns and (b) FTIR spectra of Fe_3O_4, Fe_3O_4@SiO_2 and Fe_3O_4@SiO_2–SO_3H. Patterns are offset for clarity.

The physisorption of nitrogen resulted in an isotherm of the type IV. The BET surface area was 138 $m^2\ g^{-1}$ for the final catalyst, compared to 62 $m^2\ g^{-1}$ for the bare magnetite, and had a pore volume of 0.31 $cm^3\ g^{-1}$ and a mean pore width of 8.9 nm. As expected from the increase in the non-magnetic mass, the saturation magnetisation has decreased from 61.3 emu g^{-1} (Fe_3O_4) to 41.5 emu g^{-1} (Fe_3O_4@SiO_2) and 33.8 emu g^{-1} (final catalyst), and there was no coercivity detected, indicating that the particles are superparamagnetic. Nevertheless, the catalyst was in 20 s removed from the reaction mixture with a hand magnet. The sulfur content of the CHNS analysis was 3.5 wt% (1.12 mmol $H^-\ g^{-1}$), which is reasonably consistent with the titration result. This indicates that almost all grafted sulfur was oxidised to accessible sulfonic acid groups.

3.2 Optimisation of reaction conditions

The Biginelli condensation of benzaldehyde, ethyl acetoacetate and urea to obtain 4a was chosen as the model reaction (Table 1; Graph 1). In the absence of the catalyst, only 9% of 4a was obtained in 30 min and in 120 min, the yield was only 24%. Bare Fe_3O_4 gave 36% and Fe_3O_4@SiO_2 gave 44% which is probably due to the weak interaction of the surface hydroxyl groups with the carbonyl compounds through hydrogen bonding. The introduction of the sulfonic acid groups altered the scene completely, and 10 mg of Fe_3O_4@SiO_2–SO_3H were able to achieve a 95% yield in the same 30 min.

Table 1. Optimisation of the model reaction (benzaldehyde, ethyl acetoacetate and urea) to give 4a. Isolated yields. SF = solvent-free.

Entry	Catalyst	Amount (mg)	Solvent	Temp. (°C)	Time (min)	Yield (%)
1	None	–	SF	90	30	9
2	Fe_3O_4	10	SF	90	30	36
3	Fe_3O_4@SiO_2	10	SF	90	30	44

Annual Methodological Archive Research Review
http://amresearchreview.com/index.php/Journal/about
Volume 4, Issue 3 (2026)

Online ISSN 3007-3197
Print ISSN 3007-3189

http://amresearchreview.com/index.php/Journal/about

Entry	Catalyst	Amount (mg)	Solvent	Temp. (°C)	Time (min)	Yield (%)
4	Fe_3O_4@SiO_2–SO_3H	5	SF	90	30	78
5	Fe_3O_4@SiO_2–SO_3H	10	SF	90	30	95
6	Fe_3O_4@SiO_2–SO_3H	15	SF	90	30	95
7	Fe_3O_4@SiO_2–SO_3H	20	SF	90	30	94
8	Fe_3O_4@SiO_2–SO_3H	10	SF	50	30	54
9	Fe_3O_4@SiO_2–SO_3H	10	SF	70	30	82
10	Fe_3O_4@SiO_2–SO_3H	10	SF	110	30	93
11	Fe_3O_4@SiO_2–SO_3H	10	Ethanol	78	60	84
12	Fe_3O_4@SiO_2–SO_3H	10	Water	100	60	61
13	Fe_3O_4@SiO_2–SO_3H	10	EtOH–H_2O (1:1)	80	60	79
14	HCl (2 drops)	–	Ethanol	78	240	68

Entry 5 gives the optimised conditions. Entry 14 is the conventional procedure.
The effect of the catalyst loading up to 10 mg per mmol (Graph 1a) was observed. The yield rose from 78% at 5 mg to 95% at 10 mg, stayed at 95% at 15 mg and was 94% at 20 mg. At higher acid loads (>10 mg), acid sites become nonlimiting. The small decrease at 20 mg is within experimental error, but a greater quantity of solid could also cause the molten mixture to be more difficult to stir. The temperature response was similar (Graph 1b). As the temperature is increased the yield went up to 54% at 50 °C and further increased to 95% at 90 °C, dropped slightly to 93% at 110 °C, which is following with the thermal decomposition of the urea and generation of side products at high temperature. We therefore chose 10 mg and 90 °C.

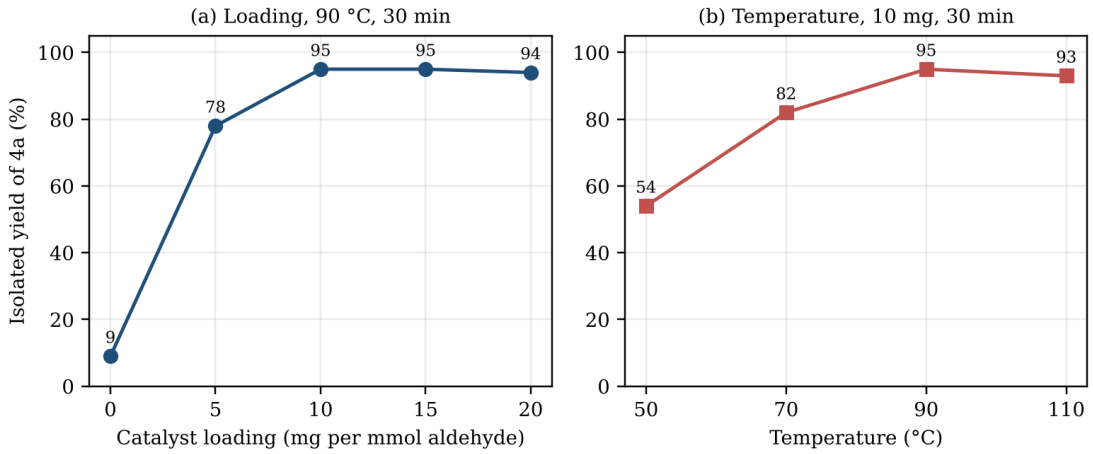

Graph 1. Effect of (a) catalyst loading at 90 °C and (b) reaction temperature at 10 mg of catalyst on the isolated yield of 4a after 30 min.
The conditions without solvents were definitely optimum (entries 5 and 11-13). After 60 min, ethanol produced 84%, the ethanol–water mixture 79% and pure water 61%.

Annual Methodological Archive Research Review
http://amresearchreview.com/index.php/Journal/about
Volume 4, Issue 3 (2026)

Online ISSN 3007-3197
Print ISSN 3007-3189
http://amresearchreview.com/index.php/Journal/about

The concentration of reactant is lower (dilute) in the solvent and the polar solvent molecules interact with the surface acid sites (coordination holes) reducing their acidity. The reactant concentration is lower (dilute), and the polar solvent molecules interact with the surface acid sites (coordination holes), which decreases their acidity and slows the condensation. Also, the solvent has the greatest proportion of the waste mass and its removal follows the rationale of current solvent guides (Jordan et al., 2022). The new system yielded 27 percentage points more than the conventional HCl/ethanol system (entry 14) and in one eight of the time. The turnover number was approximately 85 and the turnover frequency approximately 170 h-1 when the concentration of acid sites was 0.0112 mmol per run.

3.3 Substrate scope

Twelve DHPMs were obtained under the optimised conditions (Table 2) with nine aromatic aldehydes and three with thiourea. The highest yields and the lowest reaction times were obtained for aldehydes with electron withdrawing groups. The 4-chloro, 4-nitro, 3-nitro and 4-bromo derivatives (4b, 4c, 4h, 4i) were obtained in 93–97% (mean 95.0%) in 20–25 min, while the electron-rich 4-methoxy, 4-methyl and 4-hydroxy derivatives (4d, 4e, 4f) needed 35–45 min and gave 88–92% (mean 90.0%). This follows a mechanism in which the first step is attack of the urea on a protonated aldehyde, which is more readily accomplished by a more electrophilic carbonyl. The free phenolic hydroxyl group in 4f remained intact, indicating that the acid catalyst is not affected by this functional group. The ortho substituted 2-chlorobenzaldehyde 4g was slower and less efficient (89% in 40 min) than the para isomer 4b (94% in 25 min) probably for steric reasons. Thiourea was less reactive than urea, requiring longer times than any of the urea analogues 4a, 4b and 4d (mean 90.0%, mean 43.3 min). This may be because the partner of sulfur is less nucleophilic in strongly acidic environments, but we did not directly test this.

Table 2. Synthesis of 3,4-dihydropyrimidin-2(1H)-ones and thiones (4a–4l) catalysed by Fe_3O_4@SiO_2–SO_3H under solvent-free conditions at 90 °C.

Compound	Ar	X	Time (min)	Yield (%)	m.p. (°C)
4a	C_6H_5	O	30	95	202–204
4b	4-ClC_6H_4	O	25	94	213–215
4c	4-$NO_2C_6H_4$	O	20	97	207–209
4d	4-$CH_3OC_6H_4$	O	40	90	201–203
4e	4-$CH_3C_6H_4$	O	35	92	214–216
4f	4-HOC_6H_4	O	45	88	227–229
4g	2-ClC_6H_4	O	40	89	215–217
4h	3-$NO_2C_6H_4$	O	20	96	227–229
4i	4-BrC_6H_4	O	25	93	214–216
4j	C_6H_5	S	40	91	207–209
4k	4-ClC_6H_4	S	35	93	190–192
4l	4-$CH_3OC_6H_4$	S	55	86	151–153

Annual Methodological Archive Research Review
http://amresearchreview.com/index.php/Journal/about
Volume 4, Issue 3 (2026)

Online ISSN 3007-3197
Print ISSN 3007-3189
http://amresearchreview.com/index.php/Journal/about

Conditions: aldehyde (1 mmol), ethyl acetoacetate (1 mmol), urea or thiourea (1.2 mmol), catalyst (10 mg). Yields are isolated yields after recrystallisation.

The products were identified from their spectra. For the model compound 4a, FTIR showed N–H stretches at 3238 cm^{-1}, an ester C=O band at 1722 cm^{-1} and an amide C=O band at 1648 cm^{-1}. The ^{1}H NMR spectrum (DMSO-d_6) contained singlets for the two N–H protons at δ 9.19 and 7.73, a multiplet for the five aromatic protons at δ 7.36–7.22, a doublet for H-4 at δ 5.15 (J = 3.2 Hz), the ethyl ester signals at δ 3.98 (q) and 1.09 (t), and the 6-methyl singlet at δ 2.25. The ^{13}C NMR spectrum showed 12 signals, including the ester carbonyl at δ 165.7 and the C-4 methine at δ 53.9. These values agreed with those reported for this well-known compound.

3.4 Proposed mechanism

The results are consistent with the N-acyliminium route (Kappe, 1997) in which the catalyst is a Brønsted acid. Protonation of the aldehyde carbonyl and addition of urea, first; and subsequently the N-H bonds of the hydrazones are replaced by the more polar alcohol and amine carbonyl groups, respectively. An N-acyliminium ion is the intermediate which determines the rate when water is lost. Secondly, the enol form of ethyl acetoacetate reacts with the iminium carbon to give an open chain ureide. Third, the carbonyl group of the ketone undergoes the attack of the free NH_2 group and the ring is closed by dehydration to yield the DHPM. Even the non-sulfonated silica-coated particles were moderately active (entry 3), suggesting that these groups may assist to keep the reactants in close proximity to the acid sites via hydrogen bonding.

3.5 Reusability, leaching and stability

In the model reaction (Graph 2) the catalyst was used repeatedly eight times. The yield remained constant at 95% for the first 2 cycles, and then decreased slightly to 93%, 94% and 91% in cycles 6, 7 and 8 respectively. Gravimetric recovery after each cycle was 98%, 92% in the first run and the 8th run respectively. The yield of a hot filtration experiment after 10 min was 41%. At this time removal of the catalyst resulted in a supernatant of only 43%, while the control with catalyst had a superior of 95% after 20 minutes. Iron and sulfur were measured, after the first cycle, by ICP-OES and the concentrations were 0.4mg/L of Fe and 1.9mg/L of S. These data show that catalysis takes place on the solid and that leaching is negligible.

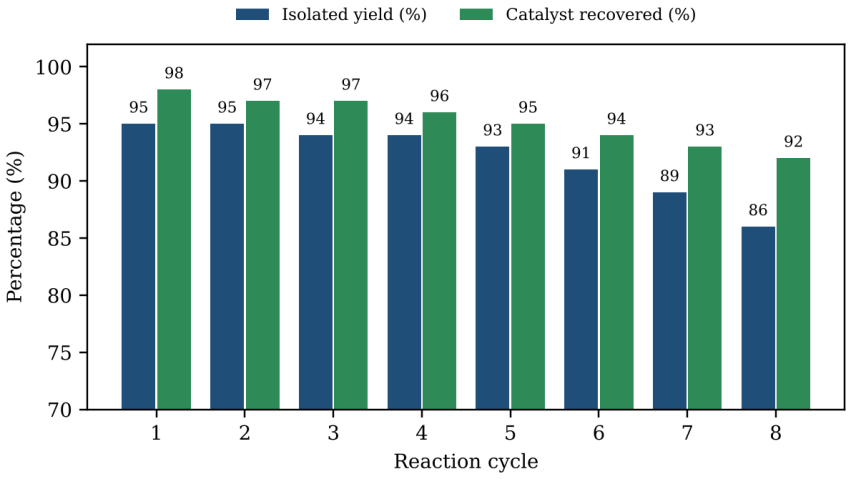

Annual Methodological Archive Research Review
http://amresearchreview.com/index.php/Journal/about
Volume 4, Issue 3 (2026)

Online ISSN 3007-3197
Print ISSN 3007-3189
http://amresearchreview.com/index.php/Journal/about

Graph 2. Reusability of Fe_3O_4@SiO_2–SO_3H in the synthesis of 4a over eight cycles: isolated yield and gravimetric catalyst recovery.

The reduction in activity is attributed to changes in the catalyst after 8 cycles, which is attributed to a slow loss in activity. The acid capacity decreased from 1.12 to 0.97 mmol H^+ g^{-1} (a 13% loss), the BET surface area from 138 to 121 m^2 g^{-1}, and the saturation magnetisation from 33.8 to 31.9 emu g^{-1}. The XRD pattern of the used catalyst remained the same, and the TEM image revealed a less significant aggregation with a core–shell structure. The decrease is probably due to progressive loss of some propylsulfonic groups due to hydrolysis and to adsorption of organic impurities on the surface. The difference in yield between the first and eighth run is 9 points, which compares favorably with the loss of acid sites (13%). This indicates that there are some excess acid sites in the selected loading.

3.6 Green metrics

The atom economy of the condensation of benzaldehyde, ethyl acetoacetate and urea (total mass = 296.32 g mol-1) to yield 4a (260.29 g mol-1) and 2 mol of water is 87.8%. As the reaction is solvent free, the E factor of the reaction was only 0.25. Including the 2 mL of ethanol used for work-up, the E-factor of the whole procedure was 6.6, the PMI was 7.6 and the RME was 80.2%. The conventional HCl/ethanol process had an E-factor of 63.2, a PMI of 64.2 and an RME of 57.4%, which used 14 mL of ethanol, with a lower yield. The new method thus reduces the E-factor by almost 9.5 times. The purification method used results in about 96% of the remaining mass being recrystallisation ethanol, which is the next improvement to consider if purity is not an issue, given that the process is direct. This has not been tested. The metrics also exclude the energy demand and also do not include the solvent used during catalyst preparation (toluene in the grafting step) and a complete life cycle assessment would have to be used to determine the overall impact.

3.7 Cytotoxic and antibacterial activity

Two of these were tested against cytotoxicity on MCF-7 cells while the other seven products were tested for their antibacterial activity (Table 3; Graph 3). The activity of all the compounds was in the micromolar range, ranging from IC_{50} = 9.8 µM to IC_{50} = 52.3 µM. The most potent compound was the thiourea derivative 4k (9.8 ± 0.6 µM), followed by the nitro derivatives 4c (15.7 ± 0.9 µM) and 4h (18.9 ± 1.1 µM). Compound 4k proved to be 3.9 times more potent than 4a ($p < 0.001$), and more potent than 4c ($p < 0.01$). It was still approximately 8 times less active than doxorubicin (1.2 ± 0.1 µM), which makes these compounds more suitable as starting points than as lead compounds.

Table 3. Cytotoxicity against MCF-7 cells (IC_{50}, mean ± SD, n = 3) and minimum inhibitory concentrations (MIC) of selected DHPMs.

Compound	IC_{50} MCF-7 (µM)	MIC *S. aureus* (µg mL^{-1})	MIC *E. coli* (µg mL^{-1})
4a	38.6 ± 2.1	32	64
4b	21.4 ± 1.3	16	32
4c	15.7 ± 0.9	8	16
4d	52.3 ± 2.8	64	128

Annual Methodological Archive Research Review
http://amresearchreview.com/index.php/Journal/about
Volume 4, Issue 3 (2026)

Online ISSN 3007-3197
Print ISSN 3007-3189
http://amresearchreview.com/index.php/Journal/about

Compound	IC_{50} MCF-7 (μM)	MIC *S. aureus* (μg mL⁻¹)	MIC *E. coli* (μg mL⁻¹)
4h	18.9 ± 1.1	16	32
4i	24.8 ± 1.5	16	32
4j	27.5 ± 1.7	32	64
4k	9.8 ± 0.6	8	16
4l	41.0 ± 2.4	64	128
Doxorubicin	1.2 ± 0.1	–	–
Ciprofloxacin	–	1	0.5

– = not tested.

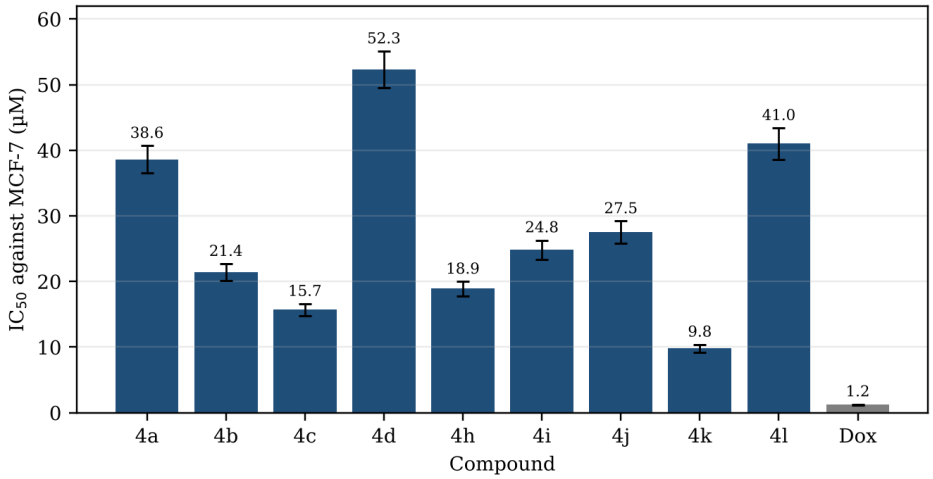

Graph 3. Cytotoxicity (IC_{50} ± SD) of selected DHPMs and doxorubicin (Dox) against MCF-7 cells.

A few observations regarding structure–activity can be made from the data. The presence of electron withdrawing groups on the ring enhanced activity in the first place. All of the halogenated and nitro substituted compounds 4b, 4c, 4h and 4i exhibited IC_{50} values below 25μM, while the methoxy group 4d, an electron-donating group, led to higher IC_{50} value of 52.3μM. Secondly, the activity of the C=O compounds was increased in all three matched pairs (compounds 4j and 4a; 4k and 4b; 4l and 4d), with the greatest improvement for the 4-chlorophenyl substitution (21.4 to 9.8 μM, 2.2-fold increase). Both features seemed to impact the effect in a more additive way, as 4k was the most powerful when both features were present.

The same order was obtained with the antibacterial effects. All the compounds were found to be twice as active against Gram positive S. aureus as compared to the Gram negative E. coli, possibly due to the outer membrane of Gram negative bacteria. However, the lowest MIC values were for compounds 4c and 4k, which were at 8 and 16 μg mL⁻¹, respectively, but were still higher than the 1 and 0.5 μg mL⁻¹ for ciprofloxacin. The activity of monastrol and other DHPMs is associated with Eg5 inhibition (Mayer et al., 1999) and the compounds described here have the same dihydropyrimidine core. This target was not tested in our assays and the mechanism of

Annual Methodological Archive Research Review
http://amresearchreview.com/index.php/Journal/about
Volume 4, Issue 3 (2026)

Online ISSN 3007-3197
Print ISSN 3007-3189
http://amresearchreview.com/index.php/Journal/about

the cytotoxic effect is unknown.

4. General Discussion

4.1 Position relative to earlier Biginelli catalysts

The Biginelli reaction was much more efficient than the classic hydrochloric acid reaction, with the use of homogeneous Lewis acids, such as indium(III) chloride (Ranu et al., 2000) and lanthanide triflates (Ma et al., 2000), and was shown to be solvent-free. The most challenging aspect of them is the practicality. The metal salt dissociates on work-up and is difficult to be recovered in an active form. While retaining the benefits of solvent-free operation, the catalyst described here is also a solid Brønsted acid and can be easily separated from the product stream using a magnet and, after suitable pretreatment, be reused. No experiments were performed with these previously reported catalysts under identical conditions. Therefore no claim is made that the present material is more active than any of these other materials. Comparing with the same scale as the classical HCl procedure is a fair comparison to use for waste, time and yield; but that is only one of the points of comparison.

4.2 Design features that appear to matter

It appears that three structural features of the catalyst are responsible for its behaviour. The magnetite core provides quick separation and the superparamagnetic nature of the magnetite particles ensures that the particles are not magnetized and do not aggregate in the absence of the magnet. The silica shell protects the core and provides anchoring points for the organosilane, which is in line with the overall concept of magnetite as a support for recyclable catalysts (Gawande et al., 2013; Wang & Astruc, 2014). The propylsulfonic acid group is then highly Brønsted acidic at a well-defined density. The division of labour is confirmed by the control experiments shown in Table 1. The core alone or the core with silica shell yielded only 36 % and 44 % respectively while the acid modified material resulted in 95 %. It also suggests that after eight cycles the link between the silica surface and the sulfonic acid chain is the weakest link, suggesting that the covalent linkage is insufficient to maintain the silica skeleton. A less hydrolysis-resistant linkage would be a good target for a second generation catalyst.

4.3 Relevance for compound libraries

Many aldehydes containing electron-rich, electron-poor and ortho-substituted and hydroxylated groups were also found to be compatible with the reaction and the products crystallise from the work-up solvent without chromatography, so the method is suitable for the rapid preparation of small DHPM libraries. This is important in medicinal chemistry, where the ease with which the scaffold can be varied and screened is crucial for the value of the multicomponent reaction (Dömling et al., 2012; Kappe, 2000). In the current data set, two clear structure–activity trends were clearly visible even in a library of 12 compounds and the best compound was synthesized in 93% yield in 35 min. It would be logical to move to a broader range of aldehyde, β-ketoesters and amidine building blocks.

4.4 Scale-up and sustainability considerations

The amount of catalyst used is modest (10 mg/mmol) and can be recovered 92-98% in every cycle. There are still a number of challenges that need to be resolved to make the method commercially viable. Reactions that are solvent-free will proceed as a melt and will have different reactions with heat and mass transfer between a large reactor and a

Online ISSN 3007-3197
Print ISSN 3007-3189
http://amresearchreview.com/index.php/Journal/about

small tube. The flow arrangement or the high gradient magnetic filter should be used for magnetic separation if the amount of material is in kilogram scale. The production of the catalyst itself uses ammonia, TEOS (organosilane), and toluene and hydrogen peroxide; therefore, the amount of catalysis needs to be balanced by the number of times it can be used. Because the catalyst is considered a recovered material and not produced, our metrics gloss over the production of the catalyst, which is a positive effect and is the reason for describing the environmental benefit as a reduction in reaction and work-up waste and not as a sustainability assessment. Taken together, the overall picture suggests that, beyond yield and atom economy, green synthesis should be evaluated by several metrics (Constable et al., 2002; Sheldon, 2017).

5. Conclusions

Twelve dihydropyrimidinones and thiones were obtained with 86–97% yields in 20–55 min with the help of a magnetic Fe_3O_4@SiO_2–SO_3H nanocatalyst without using any solvent. The catalyst was recovered by a magnet in just a few seconds and proved to be effective for 8 uses, with a decrease in yield from 95% to 86% and no significant amounts of leaching. The method was more efficient than the conventional HCl/ethanol method with one eighth of the reaction time, lower E-factor (around 9.5) and higher atom economy (87.8%). In preliminary assays, the presence of electron withdrawing groups on the aryl ring and a thiocarbonyl group enhanced both cytotoxic and antibacterial activity, and 4k was the most effective compound with an IC_{50} of 9.8 µM against MCF-7 cells.

There are some limitations to the study. All reactions were carried out at a scale of 1 mmol; the process of preparing the catalyst itself was not evaluated using life-cycle tools; the rest of the waste consists of a large proportion of recrystallisation solvent. One cancer cell line was used for the biological screening, a selectivity index was not included and the mechanism was not examined. Scale-up, chromatography-free and solvent-reduced isolation, recovery of used catalysts and target-based assays and selectivity testing should thus be studied in the future.

References

Anastas, P. T., & Eghbali, N. (2010). Green chemistry: Principles and practice. *Chemical Society Reviews, 39*(1), 301–312.

Anastas, P. T., & Warner, J. C. (1998). *Green chemistry: Theory and practice*. Oxford University Press.

Baig, R. B. N., & Varma, R. S. (2013). Magnetically retrievable catalysts for organic synthesis. *Chemical Communications, 49*(8), 752–770.

Biginelli, P. (1891). Ueber Aldehydureide des Acetessigäthers. *Berichte der Deutschen Chemischen Gesellschaft, 24*(1), 1317–1319.

Brunauer, S., Emmett, P. H., & Teller, E. (1938). Adsorption of gases in multimolecular layers. *Journal of the American Chemical Society, 60*(2), 309–319.

Cioc, R. C., Ruijter, E., & Orru, R. V. A. (2014). Multicomponent reactions: Advanced tools for sustainable organic synthesis. *Green Chemistry, 16*(6), 2958–2975.

Clinical and Laboratory Standards Institute. (2018). *Methods for dilution antimicrobial susceptibility tests for bacteria that grow aerobically* (11th ed., CLSI standard M07). CLSI.

Online ISSN 3007-3197
Print ISSN 3007-3189
http://amresearchreview.com/index.php/Journal/about

Constable, D. J. C., Curzons, A. D., & Cunningham, V. L. (2002). Metrics to "green" chemistry: Which are the best? *Green Chemistry, 4*(6), 521–527.

Dömling, A., Wang, W., & Wang, K. (2012). Chemistry and biology of multicomponent reactions. *Chemical Reviews, 112*(6), 3083–3135.

Gawande, M. B., Branco, P. S., & Varma, R. S. (2013). Nano-magnetite (Fe_3O_4) as a support for recyclable catalysts in the development of sustainable methodologies. *Chemical Society Reviews, 42*(8), 3371–3393.

Jordan, A., Hall, C. G. J., Thorp, L. R., & Sneddon, H. F. (2022). Replacement of less-preferred dipolar aprotic and ethereal solvents in synthetic organic chemistry with more sustainable alternatives. *Chemical Reviews, 122*(6), 6749–6794.

Kappe, C. O. (1993). 100 years of the Biginelli dihydropyrimidine synthesis. *Tetrahedron, 49*(32), 6937–6963.

Kappe, C. O. (1997). A reexamination of the mechanism of the Biginelli dihydropyrimidine synthesis. Support for an N-acyliminium ion intermediate. *The Journal of Organic Chemistry, 62*(21), 7201–7204.

Kappe, C. O. (2000). Biologically active dihydropyrimidones of the Biginelli-type: A literature survey. *European Journal of Medicinal Chemistry, 35*(12), 1043–1052.

Lagoja, I. M. (2005). Pyrimidine as constituent of natural biologically active compounds. *Chemistry & Biodiversity, 2*(1), 1–50.

Ma, Y., Qian, C., Wang, L., & Yang, M. (2000). Lanthanide triflate catalyzed Biginelli reaction. One-pot synthesis of dihydropyrimidinones under solvent-free conditions. *The Journal of Organic Chemistry, 65*(12), 3864–3868.

Massart, R. (1981). Preparation of aqueous magnetic liquids in alkaline and acidic media. *IEEE Transactions on Magnetics, 17*(2), 1247–1248.

Mayer, T. U., Kapoor, T. M., Haggarty, S. J., King, R. W., Schreiber, S. L., & Mitchison, T. J. (1999). Small molecule inhibitor of mitotic spindle bipolarity identified in a phenotype-based screen. *Science, 286*(5441), 971–974.

Mosmann, T. (1983). Rapid colorimetric assay for cellular growth and survival: Application to proliferation and cytotoxicity assays. *Journal of Immunological Methods, 65*(1–2), 55–63.

Patterson, A. L. (1939). The Scherrer formula for X-ray particle size determination. *Physical Review, 56*(10), 978–982.

Polshettiwar, V., Luque, R., Fihri, A., Zhu, H., Bouhrara, M., & Basset, J.-M. (2011). Magnetically recoverable nanocatalysts. *Chemical Reviews, 111*(5), 3036–3075.

Polshettiwar, V., & Varma, R. S. (2010). Green chemistry by nano-catalysis. *Green Chemistry, 12*(5), 743–754.

Ranu, B. C., Hajra, A., & Jana, U. (2000). Indium(III) chloride-catalyzed one-pot synthesis of dihydropyrimidinones by a three-component coupling of 1,3-dicarbonyl compounds, aldehydes, and urea: An improved procedure for the Biginelli reaction. *The Journal of Organic Chemistry, 65*(19), 6270–6272.

Rashid, H. U., Martines, M. A. U., Duarte, A. P., Jorge, J., Rasool, S., Muhammad, R., Ahmad, N., & Umar, M. N. (2021). Research developments in the syntheses, anti-inflammatory activities and structure–activity relationships of pyrimidines. *RSC Advances, 11*(11), 6060–6098.

Sheldon, R. A. (2012). Fundamentals of green chemistry: Efficiency in reaction design.

Online ISSN 3007-3197
Print ISSN 3007-3189

Chemical Society Reviews, 41(4), 1437–1451.

Sheldon, R. A. (2017). The E factor 25 years on: The rise of green chemistry and sustainability. *Green Chemistry, 19*(1), 18–43.

Stöber, W., Fink, A., & Bohn, E. (1968). Controlled growth of monodisperse silica spheres in the micron size range. *Journal of Colloid and Interface Science, 26*(1), 62–69.

Suresh, & Sandhu, J. S. (2012). Past, present and future of the Biginelli reaction: A critical perspective. *ARKIVOC, 2012*(1), 66–133.

Trost, B. M. (1991). The atom economy: A search for synthetic efficiency. *Science, 254*(5037), 1471–1477.

Wang, D., & Astruc, D. (2014). Fast-growing field of magnetically recyclable nanocatalysts. *Chemical Reviews, 114*(14), 6949–6985.